

Electronic Supplementary Information

Synthesis of an efficient far-red/near-infrared luminogen with AIE characteristic for *in vivo* bioimaging applications

Wei Qin,^{‡,a} Nuernisha Alifu,^{‡,b} Yuanjin Cai,^c Jacky W. Y. Lam,^a Xuwen He,^a Huifang Su,^a Pengfei Zhang,^a Jun Qian,^{*b} and Ben Zhong Tang^{*,a,d,e}

^a *Department of Chemistry, Hong Kong Branch of Chinese National Engineering Research Centre for Tissue Restoration and Reconstruction, Institute for Advanced Study, Institute of Molecular Functional Materials, Division of Biomedical Engineering, State Key Laboratory of Molecular Neuroscience, Division of Life Science, Hong Kong University of Science and Technology, Clear Water Bay, Kowloon, Hong Kong;* ^b *State Key Laboratory of Modern Optical Instrumentations, Center for Optical and Electromagnetic Research; JORCEP (Sino-Swedish Joint Research Center of photonics), Zhejiang University, Hangzhou 310058, China;* ^c *Beijing Advanced Innovation Center for Soft Matter Science and Engineering, Beijing University of Chemical Technology, Beijing 100029, China.* ^d *Centre for Aggregation-Induced Emission, SCUT-HKUST Joint Research Laboratory, State Key Laboratory of Luminescent Materials and Devices, South China University of Technology, Guangzhou 510640, China;* ^e *HKUST Shenzhen Research Institute, No. 9 Yuexing 1st RD, South Area Hi-tech Park, Nanshan, Shenzhen 518057 China.*

[‡] W. Q and N. A contributed equally to this work.

Table of Contents

Experimental section

Scheme S1. Synthetic routes to TTSe.

Fig. S1. ^1H NMR spectrum of TTSe in dichloromethane- d_2 .

Fig. S2. HRMS spectrum of TTSe.

Fig. S3. Normalized absorption spectra of TTSe in solvents with different polarities.

Table S1. Optical property of TTSe.

Fig. S4. Optimized geometries and molecular orbital amplitude plots of HOMO and LUMO of TTSe by the B3LYP/6-311G(d) basis set.

Fig. S5. Optimized molecular geometries of TTSe by DFT calculations using the B3LYP/6-31G(d) basis set with Grimme's Empirical Dispersion correction (GD3). Hydrogen atoms were omitted for clarity.

Table S2. Summary of torsion angles ($^\circ$) between different aromatic rings and double bonds in TTSe.

Fig. S6. The schematic illustration of the fabrication process of TTSe dots.

Fig. S7. (A) The particle size distribution of TTSe studied by DLS and (B) the absorption and emission spectra of TTSe dots suspended in water; $\lambda_{\text{ex}} = 500$ nm.

Fig. S8. The confocal images of A549 cells after incubation with 100 $\mu\text{g}/\text{mL}$ of TTSe dots for 2 h at 37 $^\circ\text{C}$. (A) Bright field, (B) fluorescence image (C) the merged image of panel (A) and (B). Scale bar: 20 μm .

Fig. S9. (A) Photostability of TTSe under continuous scanning irradiation (10% power) at 488 nm. I_0 is the initial PL intensity, while I is the PL intensity of the corresponding sample at a designated time interval. (B) Cell viability of A549 cells after incubation with 0, 5, 10, 20, 50, 100 and 200 $\mu\text{g}/\text{mL}$ of TTSe dots for 24 h.

Fig. S10. (A–D) Real-time *in vivo* fluorescence imaging of nude mouse after TTSe dots injection at different time (12–72 h). The blue circles mark the tumor sites. (E) Average PL intensity of the tumor tissues of mice treated with TTSe dots at different time (0–72 h). (F) Plot of relative fluorescence intensity (I/I_0) of TTSe dots versus time, where I_0 is the PL intensity at 0 h.

Fig. S11. (A) *Ex vivo* imaging of major organs of mice (from 1 to 7: tumor, heart, lung, liver, spleen, kidneys and bladder) after post-injection of TTSe dots for 72 h (left). A control model at the same experimental conditions (right). (B) Average PL intensity of mouse tissues after 72 h post-injection.

Experimental section

Materials and Instrumentations

4,7-bis(4-bromophenyl)-2,1,3-benzothiadiazole **1**,¹ compound **2**,² 4-bromotriphenylamine **4**,³ TPE derivative **5**⁴ and compound **6**⁵ were prepared according to the literature methods. THF was purchased from *J & K* and distilled under N₂ protection from sodium benzophenone ketyl before use. Other solvents and chemical reagents were purchased from Aldrich, *J & K* or Energy Chemical in China and were used as received without any further purification. Ultraviolet–visible spectra were carried out on a Milton Roy 5 Spectronic 3000 Array spectrophotometer. The lifetime of TTSe powders at room temperature was measured using an Edinburgh FLSP920 spectrophotometer equipped with a 450 nm picosecond pulsed diode laser (EPL-450, 5 mW). PL spectra of TTSe were measured under a Perkin-Elmer LS 55 spectrofluorometer. The quantum efficiency of TTSe in solid powders was measured on a calibrated integrating sphere at a excitation wavelength of 500 nm. The quantum efficiency of TTSe in THF solution was determined by using 4-(dicyanomethylene)-2-methyl-6-(*p*-dimethylaminostyryl)-4*H*-pyran ($\Phi_F = 43\%$ in methanol) as standard.

Synthesis

A mixture of compound **2** (312 mg, 0.75 mmol), selenium dioxide (94 mg, 0.85 mmol), ethanol (10 mL) and water (3 mL) was heated to reflux for 3 h under nitrogen. The mixture was cooled to room temperature. The yellow precipitates formed were filtered off, washed with water (200 mL) followed with ethyl acetate (10 mL) and dried to give **3** as yellow powders in 81.4% yield (301 mg). ¹H NMR (400 MHz, chloroform-*d*), δ (TMS, ppm): 7.76 (d, *J* = 4.0 Hz, 4H), 7.66 (d, *J* = 4.0 Hz, 4H), 7.62 (s, 2H). HRMS (MALDI-TOF), *m/z*: [M⁺] calcd for C₁₈H₁₀Br₂N₂Se, 493.8355; found, 493.8637.

A mixture of compound **3**, (148 mg, 0.3 mmol), *N*¹,*N*¹-diphenyl-*N*⁴-(4-(1,2,2-triphenylvinyl)phenyl)benzene-1,4-diamine **6**, (413 mg, 0.7 mmol), Cs₂CO₃ (975 mg, 3.0 mmol), Pd(OAc)₂ (27 mg, 0.12 mmol), P(*t*-Bu)₃·HBF₄ (104 mg, 0.36 mmol) and dry toluene (30 mL) was heated at 45 °C for 1 h under nitrogen. And then the reaction mixture was heated at 95 °C for 36 h. The

mixture was cooled to room temperature. After filtration, water (50 mL) and DCM (180 mL) were added. An organic layer was separated and washed with water (50 mL) three times, dried over anhydrous Na₂SO₄ and evaporated to dryness under reduced pressure. The crude product was purified by silica gel column chromatography using hexane/dichloromethane as eluent, affording a deep red solid in 54.3% yield (246 mg). ¹H NMR (400 MHz, dichloromethane-*d*₂), δ (TMS, ppm): 7.82 (d, *J* = 8.0 Hz, 4H), 7.61 (s, 2H), 7.27 (t, *J* = 7.6 Hz, 8H), 7.17–7.04 (m, 54H), 6.94 (m, 8H). ¹³C NMR (100 MHz, THF-*d*₈), δ (TMS, ppm): 160.62, 148.88, 148.29, 146.90, 145.04, 144.76, 144.59, 144.48, 143.27, 141.71, 141.65, 139.18, 134.59, 133.12, 133.02, 132.20, 132.17, 131.21, 130.00, 128.45, 128.40, 128.37, 128.05, 127.19, 127.08, 126.83, 126.04, 124.70, 123.59, 123.40, 123.36. HRMS (MALDI-TOF), *m/z*: [M⁺] calcd for C₁₀₆H₇₆N₆Se, 1513. 5330; found, 1513. 5337.

Preparation and characterization of TTSe dots: TTSe dots were fabricated by the method of nanoprecipitation method. Briefly, 0.1 mL THF solution of TTSe (1 mg) and 0.25 mL THF solution of Pluronic[®] F-127 (25 mg) were mixed under continuous sonication for 5 min in a flask (25 mL). Water (1 mL) was added under stirring and the resulting solution was sonicated until the solution to form a homogeneous solution. After THF removal by nitrogen gas, a certain volume of water was added under sonication to maintain the concentration of TTSe to 1 mg/mL based on the AIE luminogen. The mixture was filtered by a syringe filter (0.22 μ m) to yield the TTSe dots.

Cytotoxicity of TTSe: Cell viability assay based on Cell Counting Kit-8 was performed to calculate the metabolic activity of cells. A549 cells were seeded with a density of 6×10^4 cells/mL in 96-well plates. After 24 h incubation, the old medium was replaced by TTSe dots suspensions with different concentrations (0–200 μ g/mL). The cells were incubated for 24 h. Afterwards, the wells were washed with $1 \times$ PBS. CCK-8 Reagent (10 μ L) was added into each well. After 3 h incubation at 37 °C, the absorbance of CCK-8 was analyzed by the microplate reader at 450 nm. The cell viability of A549 cells was calculated by the ratio of absorbance of the cells incubated with TTSe suspensions to that of the cells incubated with blank culture medium.

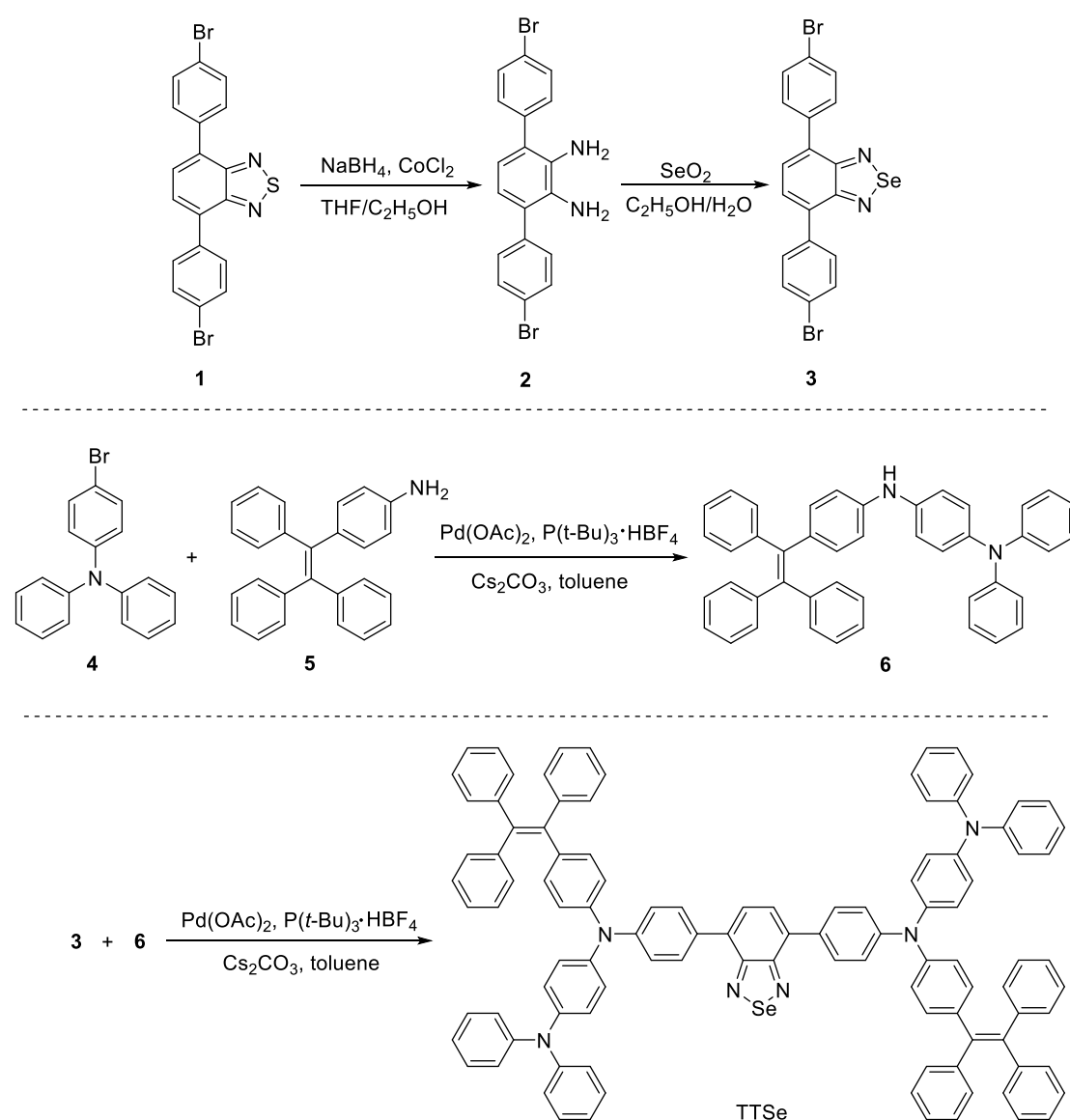
Animals: The ICR (male, 18–20 g) and nude mice (male, 18–20 g) were obtained from the Laboratory Animal Center of Zhejiang University (Hangzhou, China). The animal housing area in Animal Experimentation Center of Zhejiang University was maintained at 24 °C under a 12 h light/dark cycle, and mice were fed with standard laboratory chow and water. All *in vivo* experiments were strictly followed the guidelines and requirements of the Institutional Ethical Committee of Animal Experimentation of Zhejiang University.

In vivo sentinel lymph node mapping: For conducting the sentinel lymph node mapping of TTSe dots-treated mice, 20 μ L of TTSe dots (1 mg/mL in 1 \times PBS) was intramuscularly injected in the right forepaw pad of nude mice. Then the mice were anesthetized with pentobarbital at various time of post-injection. The sedated mice were then imaged by an IVIS Spectrum 3D small animal *in vivo* imaging system ($\lambda_{\text{ex}} = 500$ nm, $\lambda_{\text{em}} = 560\text{--}760$ nm, exposure time = 1 s). Afterwards, region-of-interests (ROI) were circled on the sentinel lymph node, and the fluorescence intensities were analyzed by a Living Image® Software 4.4.

In vivo tumor imaging: The tumor-xenografted mouse models were generated by subcutaneously injecting 5×10^6 UMUC3 cells/mouse (Human bladder cancer cell, in 0.1 mL 1 \times PBS, pH = 7.4) in the right ventral groove region of male nude mice (18–20 g, n = 4). Tumor growth was monitored every other day until the average tumor volume (tumor volume = length \times width² \times 0.5) was *ca.* 50 mm³. The tumor-bearing mice were intravenously injected with 200 μ L of TTSe dots (1 mg/mL, in 1 \times PBS), and the control mice were treated with an equal amount of saline. The control and experimental mice were then anesthetized and imaged using the IVIS Spectrum 3D small animal *in vivo* imaging system at different time post-injection ($\lambda_{\text{ex}} = 500$ nm, $\lambda_{\text{em}} = 560\text{--}760$ nm, exposure time = 1 s). Afterwards, ROI were circled on the tumor, and the fluorescence intensities were evaluated with a Living Image® Software 4.4.

In vivo imaging of brain blood vessels: A cranial window microsurgery (the mice were anesthetized and a small piece of skull was excised using a dental drill) was carried out on the mice brain. To ensure the mice live well before and after the

imaging experiments, all the operations were under sterile conditions during the surgery. For *in vivo* experiments, the mice were intravenously injected with 200 μL of TTSe dots (1 mg/mL in $1 \times \text{PBS}$). Then the mice were anesthetized and placed on an upright two-photon fluorescence scanning microscope system⁶ with their brain immobilized for imaging. The details for immobilization and imaging of *in vivo* brain blood vessels were referred to our previous work.⁷ The two-photon fluorescence signals of TTSe dots (from the mice brain) was passed by a 570 nm long pass filter and collected with a photomultiplier tube using non-descanned detection mode. The 750 μm -deep stacks for two-photon fluorescence of TTSe dots with a 5 μm step depth (10 μs /pixel, 1024×1024 pixel) were obtained.



Scheme S1. Synthetic routes to TTSe.

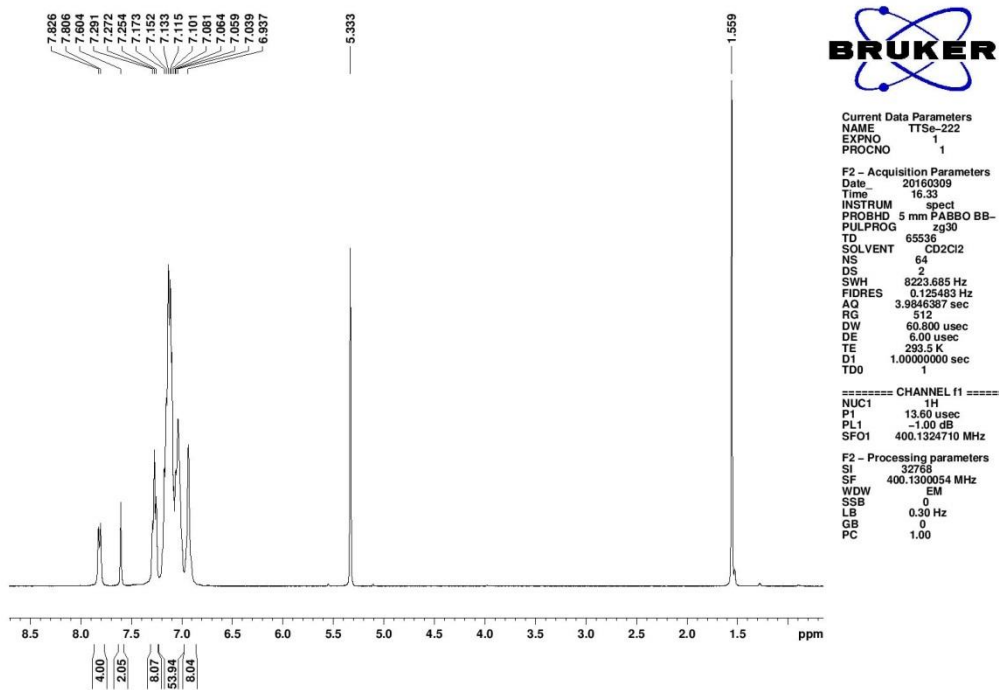


Fig. S1. ^1H NMR spectrum of TTSe in dichloromethane- d_2 .

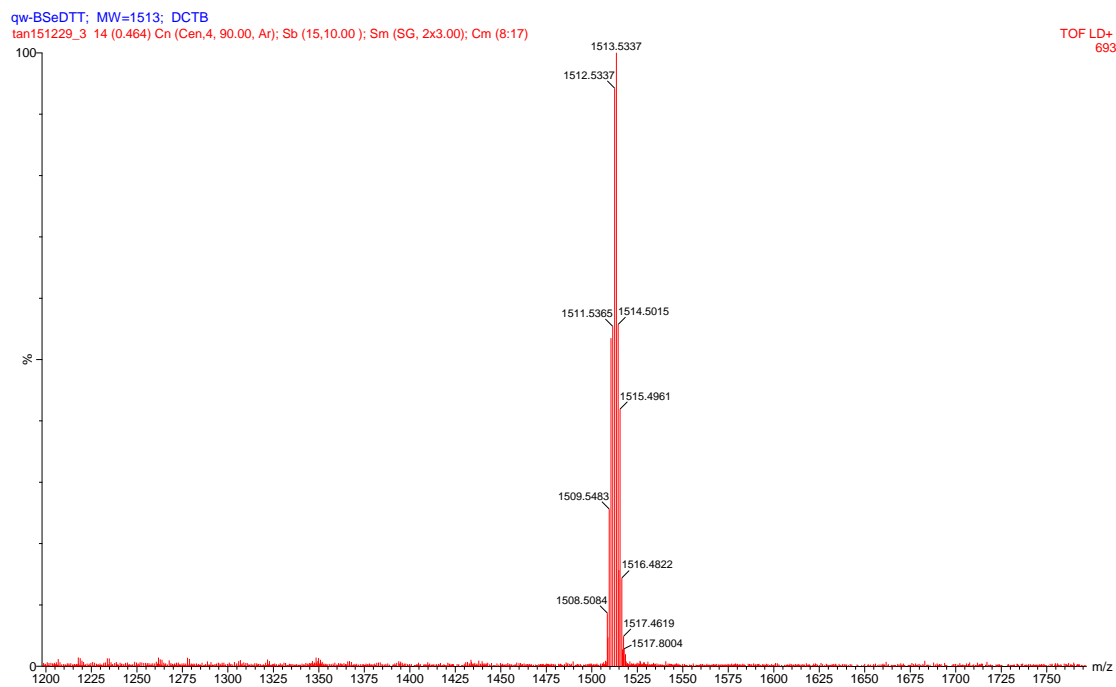


Fig. S2. HRMS spectrum of TTSe.

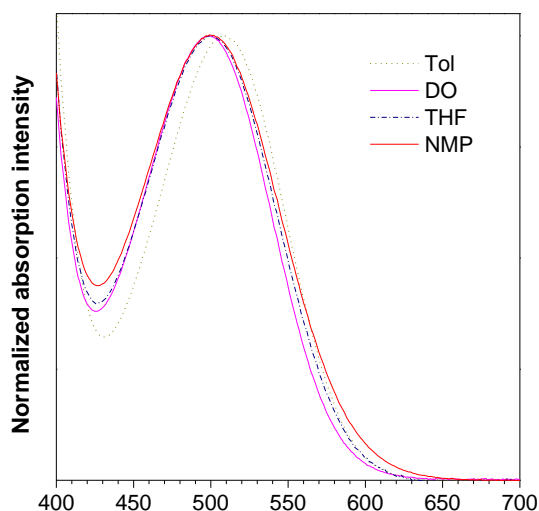


Fig. S3. Normalized absorption spectra of TTSe in solvents with different polarities.

Table S1. Optical property of TTSe.

	λ_{ab} (nm) ^a	λ_{em} (nm) ^b		τ (ns) ^d	E_{g} (eV) ^e	HOMO/LUMO(eV) ^f	
		soln (Φ_{F} ,%) ^c	aggr ^b				film (Φ_{F} ,%) ^c
TTSe	500	662 (0.01)	665	665 (8.0)	1.55	2.12 (2.15)	-4.95 (-4.49) / -2.83 (-2.34)

^a Abbreviation: λ_{ab} = absorption maximum in THF. ^b λ_{em} = emission maximum in THF solution (soln), THF/water mixture (1:9 by volume) (aggr). ^c Fluorescence quantum yield (Φ_{F} ,%) of THF solution and solid powders given in the parentheses. ^d fluorescence lifetime of solid powders (τ). ^e E_{g} represents the energy band gap estimated from the onset of the absorption spectrum. ^f E_{HOMO} is the highest occupied molecular orbital measured from the onset oxidation potential; E_{LUMO} is the lowest unoccupied molecular orbital calculated with the equation: $E_{\text{LUMO}} = E_{\text{HOMO}} + E_{\text{g}}$; the values in the parentheses are obtained from DFT calculations.

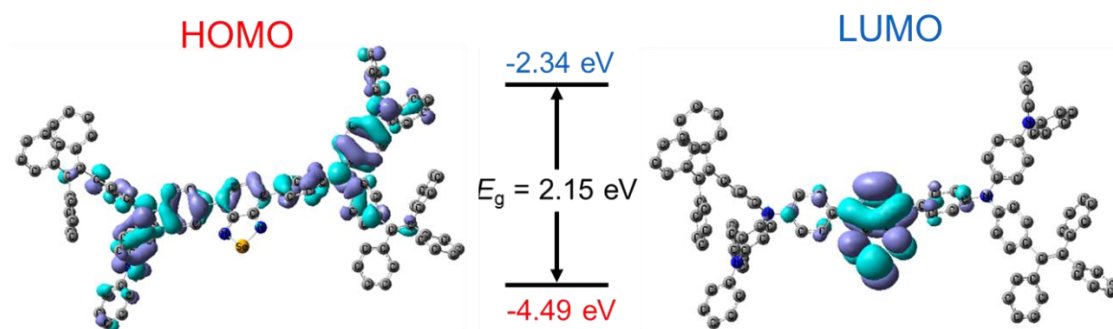


Fig. S4. Optimized geometries and molecular orbital amplitude plots of HOMO/LUMO of TTSe by the B3LYP/6-311G(d) basis set.

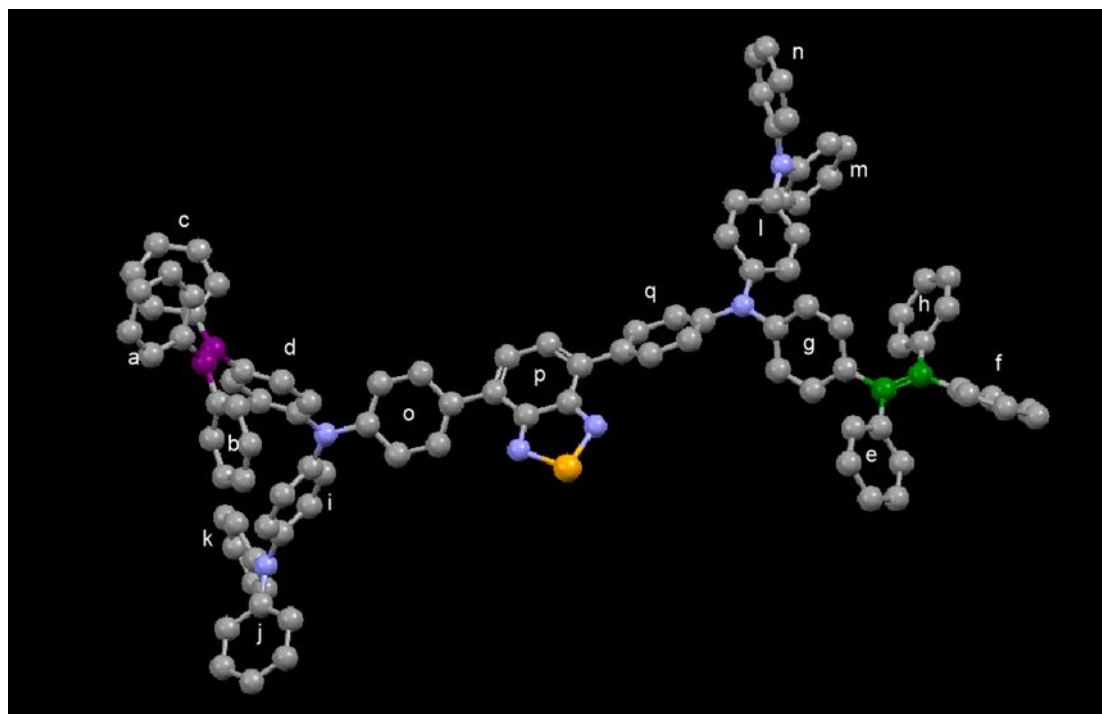


Fig. S5. Optimized molecular geometries of TTSe by DFT calculations using the B3LYP/6-31G(d) basis set with Grimme's Empirical Dispersion correction (GD3). Hydrogen atoms were omitted for clarity.

Table S2. Summary of torsion angles ($^{\circ}$) between different aromatic rings and double bonds in TTSe.

Rings and rings ^{a)}	Torsion angles ($^{\circ}$)	Rings and bonds ^{b)}	Torsion angles ($^{\circ}$)
d-o	68.36	a-dB ₁	116.55
i-o	66.81	b-dB ₁	115.35
o-p	37.38	c-dB ₁	135.25
p-q	142.64	d-dB ₁	132.42
g-q	109.08	e-dB ₂	120.79
l-q	115.95	f-dB ₂	136.23
i-j	106.56	g-dB ₂	107.38
i-k	73.70	h-dB ₂	131.19
j-k	108.06		
l-m	72.86		
l-n	73.59		
m-n	72.86		

a) a, b, c, d, e, f, g, h, i, j, k, l, m, and n represent different aromatic rings as shown in Fig. S5. d-o, i-o, o-p, p-q, g-q, and l-q are the dihedral angles between different aromatic rings. b) dB₁ and dB₂ are olefinic bonds highlighted by purple and green color, respectively, as shown in Fig. S5. a-dB₁, b-dB₁, c-dB₁, d-dB₁, e-dB₂, f-dB₂, g-dB₂ and h-dB₂ are the dihedral angles between different phenyl rings and the adjacent olefinic bonds, which are highlighted by purple and green color, respectively.

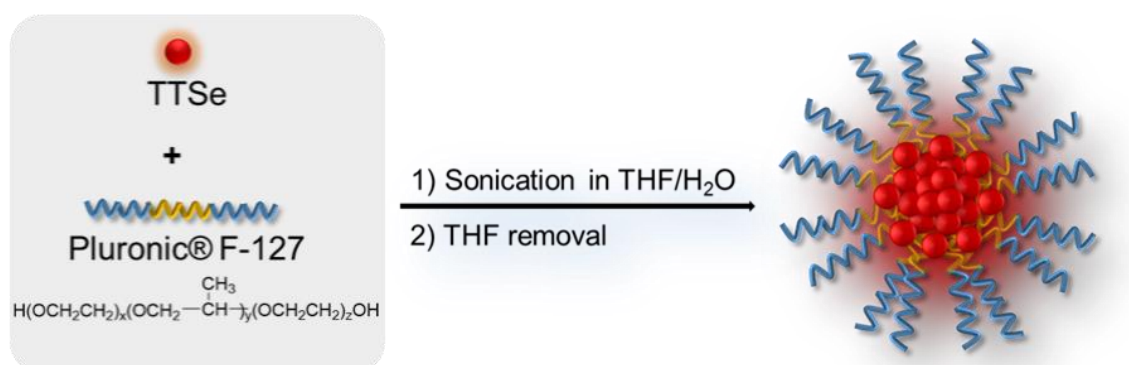


Fig. S6. The schematic illustration of the fabrication process of TTSe dots.

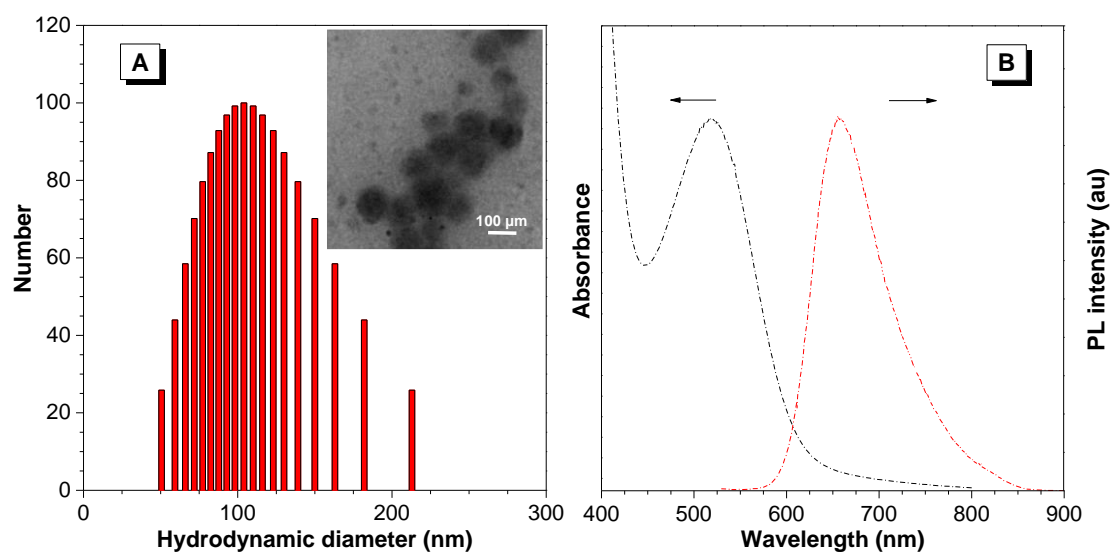


Fig. S7. (A) The particle size distribution and morphological structure of TTSe studied by DLS and (inset) high-resolution transmission electron microscopy (HR-TEM). (B) the absorption and emission spectra of TTSe dots suspended in water; $\lambda_{\text{ex}} = 500 \text{ nm}$.

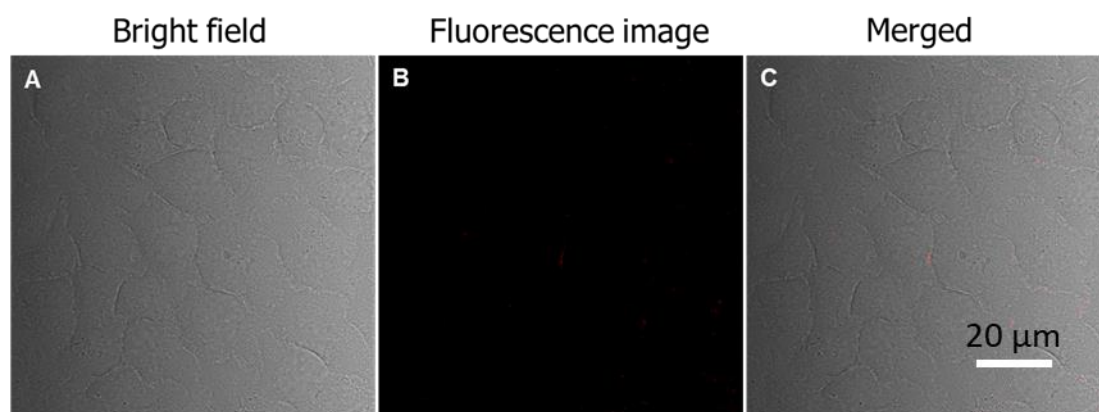


Fig. S8. The confocal images of A549 cells after incubation with 100 μg/mL of TTSe dots for 2 h at 37 °C. (A) Bright field, (B) fluorescence image (C) the merged image of panel (A) and (B). Scale bar: 20 μm.

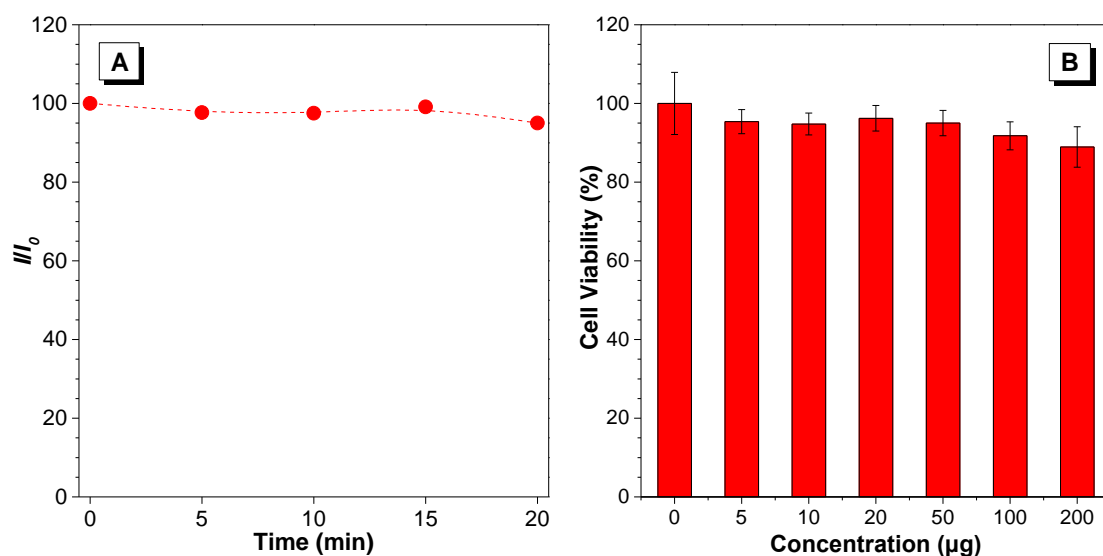


Fig. S9. (A) Photostability of TTSe under continuous scanning irradiation (10% power) at 488 nm. I_0 is the initial PL intensity, while I is the PL intensity of the corresponding sample at a designated time interval. (B) Cell viability of A549 cells after incubation with 0, 5, 10, 20, 50, 100 and 200 $\mu\text{g}/\text{mL}$ of TTSe dots for 24 h.

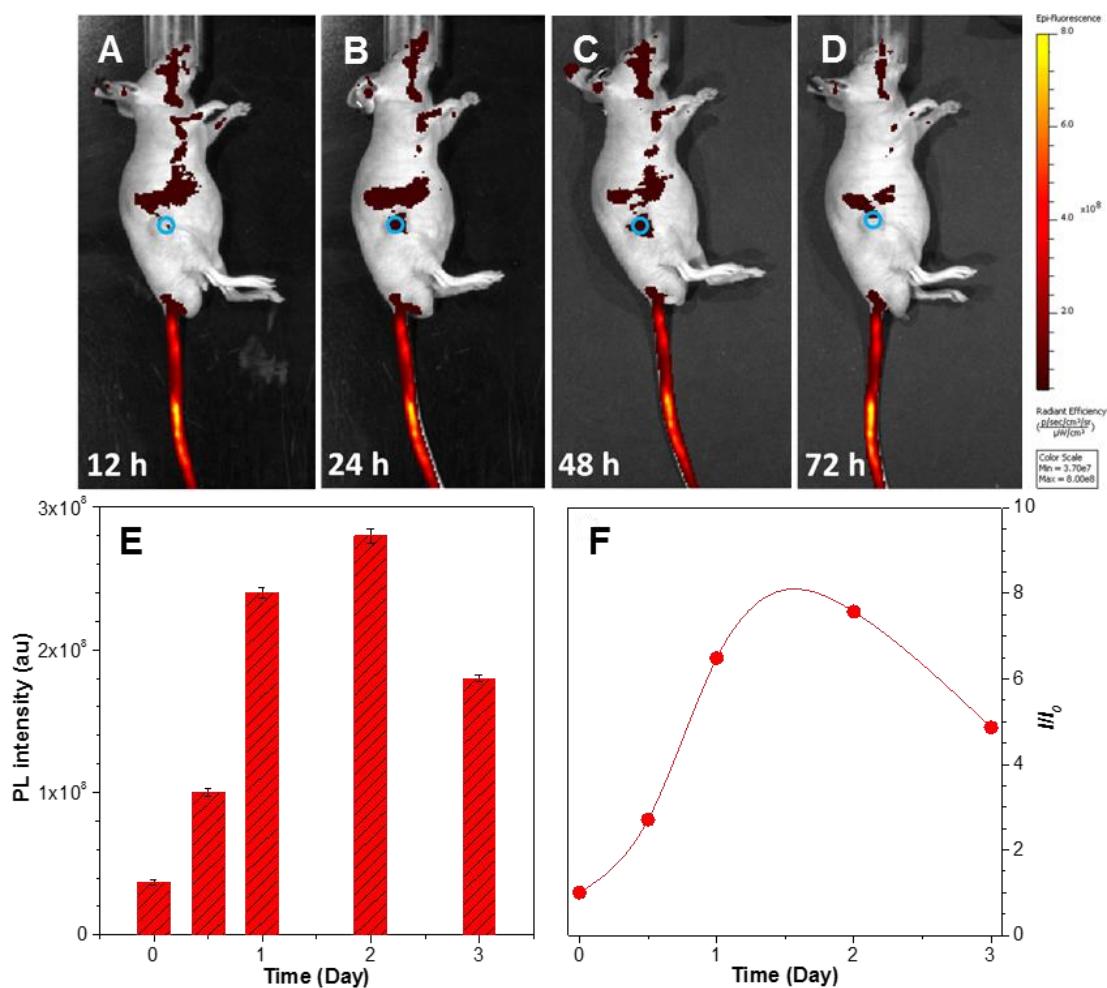


Fig. S10. (A–D) Real-time *in vivo* fluorescence imaging of nude mouse after TTSe dots injection at different time (12–72 h). The blue circles mark the tumor sites. (E) Average PL intensity of the tumor tissues of mice treated with TTSe dots at different time (0–72 h). (F) Plot of relative fluorescence intensity (I/I_0) of TTSe dots versus time, where I_0 is the PL intensity at 0 h.

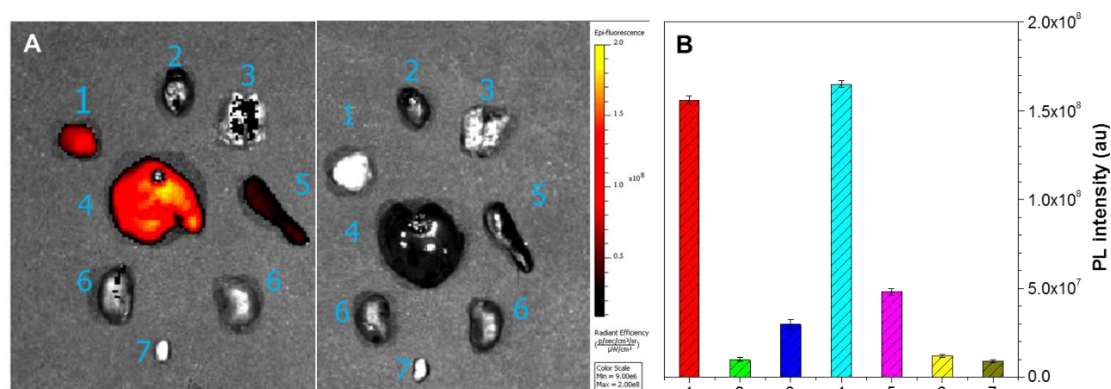


Fig. S11. (A) *Ex vivo* imaging of major organs of mice (from 1 to 7: tumor, heart, lung, liver, spleen, kidneys and bladder) after post-injection of TTSe dots for 72 h (left). A control model at the same experimental conditions (right). (B) Average PL intensity of mouse tissues after 72 h post-injection.

References

1. J. Liu, L. Bu, J. Dong, Q. Zhou, Y. Geng, D. Ma, L. Wang, X. Jing and F. Wang, *J. Mater. Chem.*, 2007, **17**, 2832.
2. E. Shi, H. Zhuang, Z. Liu, X. Cheng, H. Hu, N. Li, D. Chen, Q. Xu, J. He, H. Li, J. Lu and J. Zheng, *Dyes. Pigments*, 2015, **122**, 66.
3. D. Lumpi, B. Holzer, J. Binteringer, E. Horkel, S. Waid, H. D. Wanzenbock, M. Marchetti-Deschmann, C. Hametner, E. Bertagnolli, I. Kymissis and J. Frohlich, *New J. Chem.*, 2015, **39**, 1840.
4. X. F. Duan, J. Zeng, J. W. Lü and Z. B. Zhang, *J. Org. Chem.*, 2006, **71**, 9873.
5. W. Qin, P. Zhang, H. Li, J. W. Y. Lam, Y. Cai, R. T. K. Kwok, J. Qian, W. Zheng and B. Z. Tang, *Chem. Sci.*, 2018, **9**, 2705.
6. N. Alifu, L. Yan, H. Zhang, A. Zebibula, Z. Zhu, W. Xi, A. W. Roe, B. Xu, W. Tian and J. Qian, *Dyes. Pigments*, 2017, **143**, 76.
7. J. Qian, D. Wang, F. H. Cai, W. Xi, L. Peng, Z. F. Zhu, H. He, M. L. Hu and S. He, *Angew. Chem. Int. Ed.*, 2012, **51**, 10570.